"Hydro-Gen" Trigeneration System for a Small-Medium Scale Airport: Energy and Economic Performance Assessment via Dynamic Simulations Under Electric-Load Control Strategy

Emiliano Lustrissimi[1,2]*, Bonifacio Bianco[2], Sebastiano Caravaggi[2], Luigi Maffei[1], Sergio Sibilio[1], Antonio Rosato[1]

[1] Department of Architecture and Industrial Design, RIAS Built Environment Control Laboratory, University of Campania Luigi Vanvitelli, 81031 Aversa, Italy
[2] Assing S.p.A., 00015 Monterotondo, Italy

* Correspondence: Emiliano Lustrissimi (emiliano.lustrissimi@unicampania.it)

Abstract: One of the most attractive technologies to reach the final goal of net zero emissions by 2050 lies in the use of green hydrogen that can be supplied to fuel cells for producing electricity and heat. Nowadays, airports are responsible for 13% of the European Union's transport sector greenhouse gas emissions. In this paper, an innovative containerized modular trigeneration system, named "Hydro-Gen", has been proposed to cover electric, thermal and cooling demands of a small-medium scale airport via fuel cells fuelled by green hydrogen. A dynamic simulation model of the "Hydro-Gen" system has been developed by means of the TRNSYS platform. The proposed system has been simulated under two operating scenarios with reference to a 1-year period while coupled with the selected airport demand profiles. The simulation results have been analyzed from energy and economic points of view and compared with a traditional energy generation scenario (where the central power grid only is used). The results underlined that the proposed system significantly reduces primary energy consumption under both scenarios up to a maximum 100.9%, while the economic performance are strongly dependent on the unit cost of hydrogen.

Keywords: Hydrogen; Airport; Fuel cell; Trigeneration; Energy saving

1 Introduction

Airports serve a variety of commercial, industrial, business, and entertainment purposes. An airport is a defined area on land or in water, including any buildings, installations, and equipment, that is used entirely or in part for the arrival, departure, and surface movement of aircrafts. They operate as hubs for local, national, and international transportation [1, 2]. In order to function, airports must use a lot of energy, especially electric energy; they are responsible for 13% of the European Union's transport sector greenhouse gas (GHG) emissions and 2.5% of global GHG emissions [1, 2]. As a result, there are significant opportunities to improve related energy efficiency, making them significant subjects for energy research [1–3].

Cogeneration (combined production of heat and power from a single fuel source) is considered by the European Community as one of the most effective measures to both save primary energy as well as reduce greenhouse gas emissions [4]; the combination of cogeneration systems with thermally fed or electrically-driven cooling systems allows to set up a so-called combined cooling heat and power (CCHP) system, with it representing the production in-situ of a threefold energy vector requested by the user from a single fuel source [4, 5]. One of the most attractive alternatives thermally fed technologies to be integrated into CCHP systems is represented by the adsorption chillers (ADCH) [6, 7]; adsorption cycles may operate even for supplying temperatures of 45–65℃ and a number of models are already commercialized on the market.

Cardona et al. [8] stated that CCHP systems can represent a viable solution for small airports in the case of favourable tariff scenarios. According to Calise et al. [9], one of the most promising options to handle the

unpredictability and the fluctuations typical of some renewable energy sources is represented by hydrogen, when coupled with electrolyzer, fuel cells and gas storage technologies; the EU Hydrogen Strategy seeks to encourage the widespread use of hydrogen technology in the energy sectors that are thought to be challenging to decarbonize [9, 10]. In this paper, the energy and economic feasibility of a green hydrogen-fuelled CCHP plant serving a small-medium scale airport is discussed based on detailed numerical data obtained via the TRaNsient SYSstem simulation tool (TRNSYS) [11], widely adopted in the scientific literature [9, 12, 13].

2 Selected Airport and Related Energy Demand Profiles

Energy demand of airports depends on both structural (surface, volume, characteristics of building envelope, etc.) and operational variables (number of passengers per year, occupancy profiles, etc.) related to the size of the airport; climatic conditions also play a primary role. In addition, it should be underlined that energy demands in airports can widely vary year by year, depending on variations in terms of number of passengers and/or facilities [1, 3, 8]. A feasibility study with ad hoc considerations should be conducted for every case study due to the significant variations in energy demand among airports [1, 3, 8]. However, an accurate energy and economic evaluation of the performance of a CCHP system requires a precise definition of the electrical, thermal and cooling load profiles of end-user. For this reason, a small-medium sized airport was selected as a reference in this work; in particular, the small-medium scale Seve Ballesteros-Santander airport, located 4 km south of the city of Santander in north central Spain [14] (latitude: 43°25'37" N, longitude: 03°49'12" W, altitude: 5 m) was considered in view of the fact that the aforementioned profiles were available or could be derived in the scientific literature [3]. Alba and Manana [3] reported that this airport has provided regular services to approximately 1 million passengers and 12,000 air operations per year; the main buildings and areas of this airport can be summarized as reported in Table 1.

Table 1. Main buildings, floor areas and schedules of the airport [3]

Type of Building or Area	Floor Area (m^2)	Operating Schedule
Terminal building	17,112	06:00 a.m.–11:30 p.m.
No. 1 Control tower	728	07:00 a.m.–11:30 p.m.
No. 1 Firefighting building	730	07:00 a.m.–11:30 p.m.
No. 1 Cargo terminal	636	07:00 a.m.–11:30 p.m.
No. 2 Helicopter hangars	1,700	07:00 a.m.–11:30 p.m.
No. 3 Radio navigation systems building	530	07:00 a.m.–11:30 p.m.
No. 1 Power station building	630	07:00 a.m.–11:30 p.m.
No. 1 Fuel storage building	625	07:00 a.m.–11:30 p.m.
No. 1 Parking and airport urbanization	86,900	06:00 a.m.–11:30 p.m.
Aircraft movement area (Airside)	215,980	06:00 a.m.–11:30 p.m.

Table 2. Monthly percentage energy demands of HVAC systems serving the airport as a function of the month [3]

Month	Monthly Percentage of Electric Energy Demand of HVAC Systems (%)
January	32.75%
February	33.95%
March	27.54%
April	14.73%
May	18.45%
June	31.00%
July	34.00%
August	35.26%
September	14.85%
October	12.81%
November	23.37%
December	24.90%

The electrical, thermal and cooling load profiles of the airport assumed as a reference are detailed in the following. With reference to the airport under consideration, Alba and Manana [3] suggested the total daily average quarter-hourly electric load curves (one curve per season) reported in Figure 1; the data in this figure are based on experimental measurements carried out during the year 2015. A similar curve shape can be recognized every day of a given season and, therefore, in this study it is assumed that each of the four curves shown in Figure 1 repeats

identically for all the days of the corresponding season in order to determine the total electric load profile of the year associated to the airport under consideration.
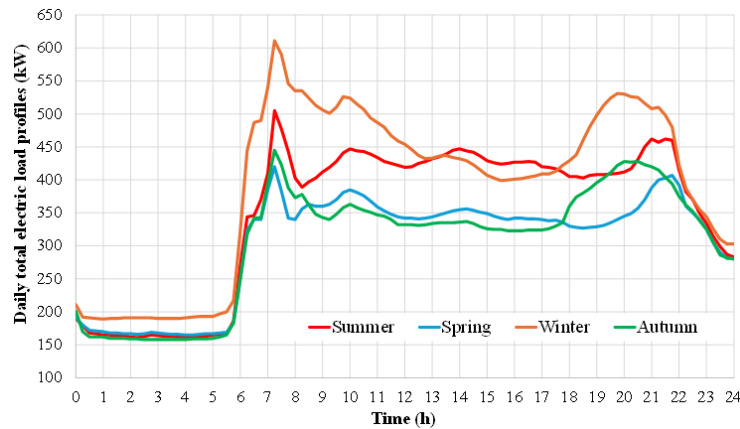

Figure 1. Daily total electric demand profiles of the airport as a function of the season [3]
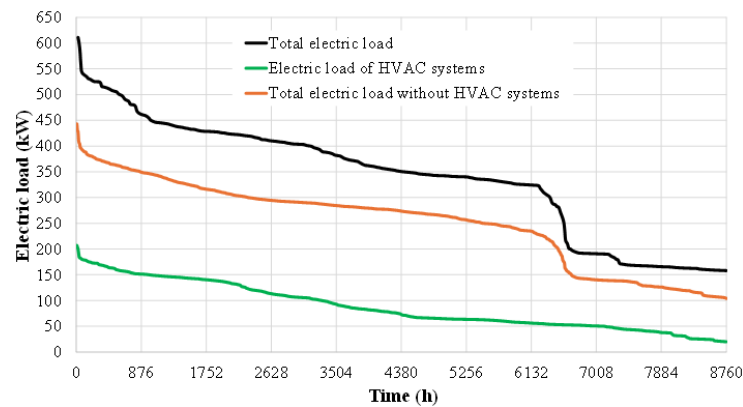

Figure 2. Yearly total and HVAC systems electric load-duration diagrams of the airport as assumed in this study
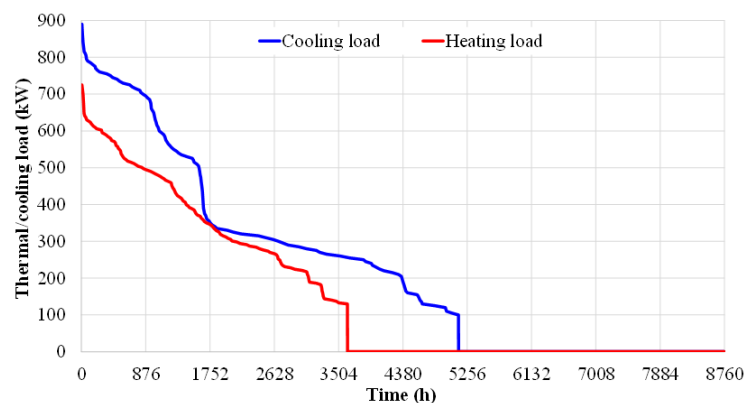

Figure 3. Thermal/cooling load-duration diagrams of the airport as assumed in this study

They also specified the percentage of monthly electrical energy demand corresponding to the operation of the Heating, Ventilation and Air-Conditioning (HVAC) systems with respect to the total electrical demand upon varying the month of the year (as indicated in Table 2). In this study, the electrical load profile associated with the operation of the HVAC systems alone was obtained by multiplying the total electrical load profile of the airport by the percentages shown in Table 2.

Figure 2 shows the total electrical power demand, the electrical power demand related to the HVAC systems, as well as the total electrical power demand without HVAC systems of the reference airport during the year assumed

728

in this study (determined as explained above). In particular, the values shown in Figure 2 are ordered in descending order with the aim of displaying the related load-duration diagrams. This figure underlines that the maximum total power demand is about 611 kW, while the power demand of HVAC systems is up to about 207 kW.

A detailed analysis of the performance of a CCHP system also requires accurate knowledge of heating and cooling load profiles of the airport (in addition to the electrical load profile). In the absence of more detailed information, in this work it has been assumed that the electrical consumption of HVAC systems serving the selected airport [3] is associated only with the use of both an electric vapor compression air-to-water heat pump to produce the hot heat carrier fluid for heating purposes during the heating period (assumed to be between November 1st and March 31st) as well as an electric vapor compression air-to-water refrigeration unit to produce the cold heat carrier fluid used for cooling purposes during the cooling period (assumed to range from April 1st to October 31st). In addition, in this work the profile of thermal power provided by the air-to-water heat pump for heating purposes during the heating period has been obtained by considering a constant seasonal coefficient of performance (SCOP) equal to 3.5 [15], while the profile of cooling power provided by the air-to-water refrigeration unit for cooling purposes during the cooling period has been obtained by considering a constant seasonal energy efficiency ratio (SEER) equal to 5.0 [16]. Figure 3 reports the thermal load profile for heating purposes and the cooling load profile for cooling purposes of the selected reference airport (with values in descending order); this figure indicates that the maximum thermal load for heating purposes is about 725 kW, while the cooling load for cooling purposes is up to about 890 kW.

3 Hydro-Gen System

In this paper an innovative containerized modular system, named "Hydro-Gen", has been designed and analyzed for generating both electric and thermal power starting from hydrogen with the aim of covering the electric, thermal and cooling demands of the airport assumed as reference in this study. The proposed system is based on fuel cells (fuelled by hydrogen) coupled with lithium battery packs, a sensible thermal energy storage connected to the fuel cells, as well as an adsorption chiller powered by the sensible thermal energy storage. The proposed system can operate either connected to the central electric grid or as stand-alone solution.

With reference to the case study under consideration and the related electrical loads described in the previous section, the "Hydro-Gen" system was assumed to consist of 2 containers with each container containing 3 modules inside. The schematic of a single container (containing 3 modules) of the "Hydro-Gen" system is reported in Figure 4.
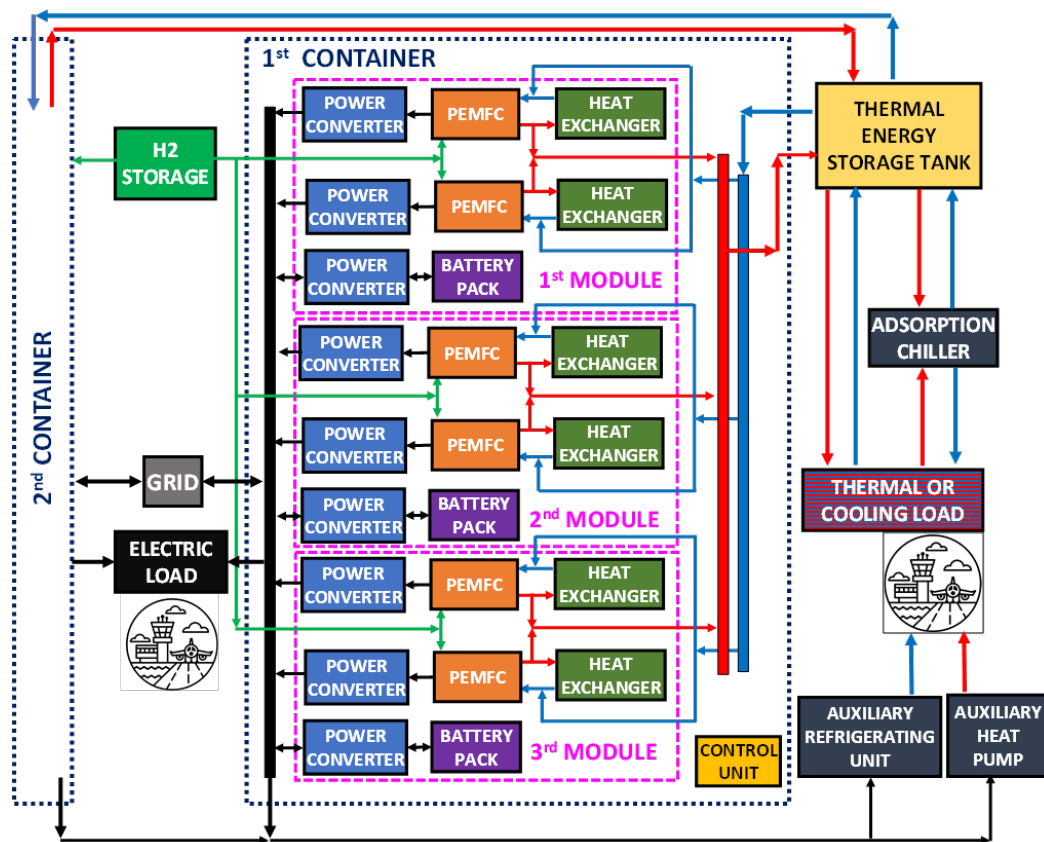

Figure 4. Schematic of the proposed "Hydro-Gen" system

Table 3. Main characteristics of the main components of the "Hydro-Gen" system

Components	Value
Proton Exchange Membrane Fuel Cells (PEMFCs)	
Number of PEMFCs per container	6
Net rated electric output of a single PEMFC (kW)	45.0
Net rated thermal output of a single PEMFC (kW)	41.3
Auxiliaries (air compressor, coolant pump) rated power demand of a single PEMFC (kW)	4.1
Heat Transfer Fluid / Coolant	
Mixture of water/ethylene glycol (% by volume)	50/50
Density (kg/m^3)	1050
Specific heat (J/kgK)	3840
Batteries	
Number of batteries per container	3 parallel-connected
Single battery capacity (Ah)	80
Single battery maximum charging power (kW)	24.6
Single battery maximum discharging power (kW)	49.2
Round-trip efficiency (%)	98.8
Heat Exchangers (HEs)	
Number of HEs per container	6
Rated fluid volumetric flowrate of a single HE (l/min)	140
Rated air volumetric flowrate of a single HE (m^3/s)	3.33
Rated fan power demand of a single HE (kW)	2.0
Sensible Thermal Energy Storage	
Volume (m^3)	24
Adsorption Chiller	
Rated cooling capacity (kW)	890
Efficiency	0.6
Auxiliary Heat Pump	
Rated thermal output (kW)	385
SCOP	3.5
Auxiliary Refrigeration Machine	
Rated cooling capacity (kW)	675
SEER	5

The main components of a single module can be summarized as follows:

• No. 2 Proton Exchange Membrane Fuel Cells (PEMFCs), powered by hydrogen and capable of producing electrical and thermal energy to meet the needs of the utility. The PEMFCs are connected to the central electricity grid and with the batteries in such a way as to allow two-way power exchange; the coolant is a mixture of water/ethylene glycol (50% / 50% by volume);

• No. 1 LiFePO4 (lithium-iron-phosphate) battery, used to store any excess eventual production of the PEMFCs and to cover the electric load in the occasional events of requests for electric power exceeding the electric power generated by the PEMFCs;

• No. 2 air-to-water heat exchangers equipped with a fan to maintain the temperature of the coolant at the outlet of the PEMFCs in a range between 70°C and 80°C. The coolant is circulated by fixed speed pumps integrated directly into the PEMFCs;

• Power DC/DC converters and AC/DC inverters to adapt the electrical voltages to the needs of the various components and convert DC to AC and vice versa. The "Hydro-Gen" system is also integrated with:

• No. 1 hydrogen storage system, where hydrogen is stored at ambient temperature and, then, through pressure reduction systems, is moved to the "Hydro-Gen" container and, then, conveyed to feed the PEMFCs;

• No. 1 sensible thermal energy storage, used to store the thermal energy produced by the PEMFCs; this thermal energy is used both to cover the needs for space heating during the heating period (assumed to be between November 1st and March 31st) and to power the adsorption chiller;

• No. 1 adsorption chiller, powered by the hot heat carrier fluid stored in the sensible thermal energy storage and used to produce the cold heat transfer fluid required for space cooling during the cooling period (assumed to range from April 1st to October 31st);

• No. 1 air-to-water electric vapor compression heat pump to supplement the thermal energy produced by the

PEMFCs and stored in the thermal energy storage if this is not enough to cover the airport's thermal needs for space heating during the heating period (assumed to be between November 1st and March 31st);

• No. 1 air-to-water electric vapor compression refrigeration machine to supplement the cooling energy production of the adsorption chiller in the cases when it is not sufficient to cover the airport's cooling energy needs during the cooling period (assumed to range from April 1st to October 31st).

Table 3 summarizes the main characteristics of the main components of the proposed "Hydro-Gen" system.

Each PEMFC has a net rated electrical power of 45.0 kW as well as a net rated thermal output of 41.3 kW (with net rated electric and thermal efficiencies equal to 46.7% and 42.9%, respectively); consequently, the "Hygro-gen" system considered in this work has a total net rated electric output of about 540 kW together with a total net rated thermal output of about 495.6 kW (being made up of 2 containers with 3 modules per each container, including 2 PEMFCs per each module). The PEMFCs are operated under electric load-following control logic at full load (without the possibility of partializing the electrical and thermal outputs) with the aim of covering (together with the batteries) the power demand due to (i) the airport without the HVAC systems (orange curve in Figure 2), (ii) the auxiliary equipment (heat exchangers' fans, PEMFCs' coolant pumps, PEMFCs' air compressors), (iii) the auxiliary heat pump, as well as (iv) the auxiliary cooling machine. Any excess electrical power produced will be fed into the batteries or the electricity grid; the central grid is also used as back-up system in case of the electric generation is lower that the power demand. Thermal power delivered by the PEMFCs is a consequence of the electrical power generated; it is stored in the sensible thermal energy storage and then used for space heating (during the heating period ranging from November 1st to March 31st) or to feed the ADHP (during the cooling period ranging from April 1st to October 31st) to satisfy the cooling demands.

4 Simulation Model of the Hydro-Gen System

In this paper a dynamic simulation model of the proposed "Hydro-Gen" system has been developed by means of the Transient Systems simulation tool (TRNSYS) version 18 [11], that is widely used in the scientific literature [17, 18]. TRNSYS consists of a number of "Types" allowing to model and simulate the behaviour of each single "Hydro-Gen" component; each TRNSYS Type is characterized by some parameters and inputs to be defined in order to calculate a number of specific outputs. Users wishing to write/modify their own components may write/modify them in Fortran, C, C++, or any other language provided that they have a compiler capable of creating a DLL. In this study, a number of TRNSYS Types have been modified in Fortran in order to more accurately model the "Hydro-Gen" components. Table 4 lists the main TRNSYS Types used to model and simulate the main "Hydro-Gen" components.

Table 4. Main TRNSYS Types used to model the "Hydro-Gen" system

Components	Value
H2 Storage	164b
Inverter AC/DC and converter DC/DC	175b
Air compressor	167
PEMFC	170d
Battery pack	549b_v2a
Single Speed Pumps	114
Variable Speed Pumps	110
Sensible thermal energy storage	158

The selected TRNSYS Types have been calibrated based on manufacturers' data; some TRNSYS Types have been modified in Fortran with respect to their original version in order to better simulate the real behaviour of the corresponding components. Figure 5 shows the diagram of the overall simulation model developed in the TRNSYS environment. With reference to the TRNSYS Type 170d, some original parameters/inputs have been modified according to the information provided by the manufacturer; in particular, the coefficients of the formula for calculating the internal electric resistance, the maximum output current as well as the management of the heat transfer fluid have been adapted to the selected PEMFC model. Figure 6 compares the values of voltage, efficiency and power suggested by the manufacturer in contrast with those simulated via the modified TRNSYS Type 170d with reference to the operation of a single PEMFC as a function of the current; the comparison highlights a good correspondence between simulated and rated values.

The batteries have been simulated via the TRNSYS Type 549b_v2a, by setting the maximum values of charging (40 A) and discharging current (80 A). Figure 7 compares the rated and simulated voltage of a single cell of the selected battery pack as a function of the Fraction State Of Charge (FSOC) under both charging and discharging phases, demonstrating a good agreement between rated and simulated values.
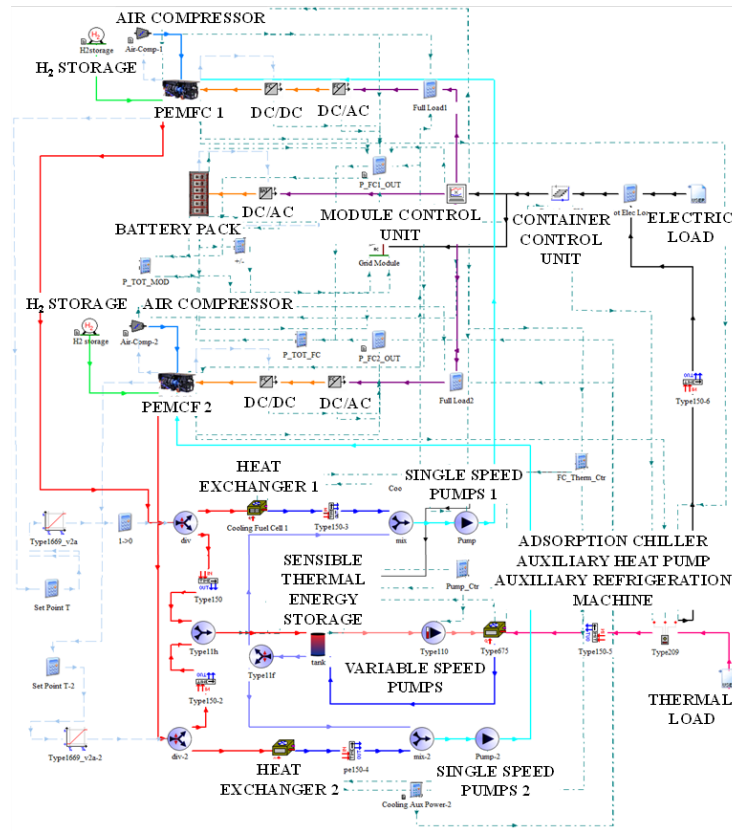
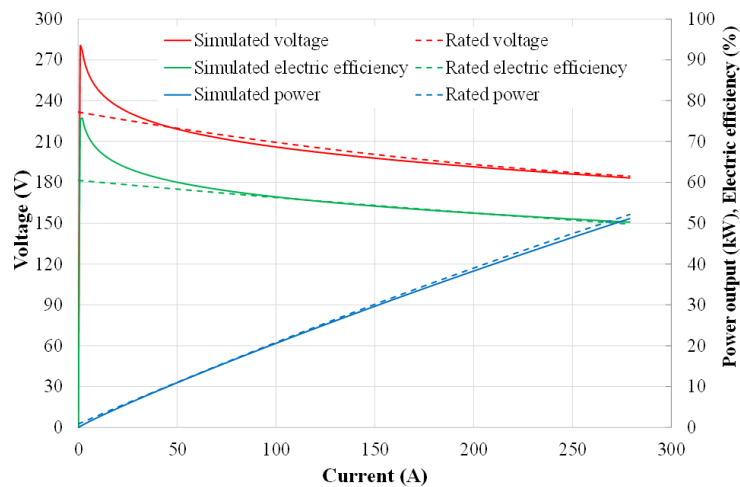**Figure 5.** TRNSYS schematic of the "Hydro-Gen" system

Figure 6. Simulated vs. rated performance of a single PEMFC

In order to cover the overall electrical load, the model requires the PEMFCs to be switched on at maximum power. The number of PEMFCs to be switched on is determined on the basis of the overall electrical demand, the state of charge of the batteries and the maximum power that can be delivered by the batteries.

In particular, the control unit will switch on a number of PEMFCs calculated by dividing the electrical demand and the rated electrical output of a single PEMFC (rounded to the lower as integer), while the complementary part (given by the difference between the overall electrical load and the generation of the active PEMFCs) is covered by the batteries. In the event that the batteries cannot actually deliver this complementary power, then the system will switch on additional PEMFCs resulting in a generation not less than the total electrical load. The batteries are charged only when there is a surplus of electrical energy generated by the PEMFCs with respect to the required electric load. In the event that there is a surplus of electrical energy generated over the load, and the batteries are already charged, the excess energy is fed back into the grid. In the model, the FSOC has been assumed ranging

between 0.15 and 0.9 during simulations, according to the manufacturer data. Battery discharging is automatically inhibited when its FSOC reaches or falls below a settable minimum level (FSOC_min) assumed equal to 0.15; battery discharging is then only re-enabled when its FSOC rises above a specified recharge value (FSOC_recharge) assumed equal to 0.5. As an example, Figure 8 shows the total electrical load, the power generated by the PEMFCs, the power charged/discharged into/from the batteries, the imported/sold power from/to the grid as well as the number of active PEMFCs (i.e., generating power) as a function of time for a typical day. The switching on of the PEMFCs and the discharging of the batteries take place as specified in the control logics described above in order to achieve a power generation equal to the total demand. The ADCH was modelled assuming a constant efficiency value of 0.6 [19] and, therefore, calculating the relative thermal power demand on the basis of this parameter and the cooling capacity required by the user for cooling needs during the cooling period only.

The thermal energy storage tank has been modelled with two inlet ports (one connected to the PEMFCs and one connected to the airport (during the heating season) or the ADCH (during the cooling season)) as well as two outlet ports (one connected to the PEMFCs and one connected to the airport (during the heating season) or the ADCH (during the cooling season)); the tank is divided into five isothermal layers. The auxiliary vapor compression electric heat pump was modelled assuming a constant SCOP value of 3.5 and, therefore, calculating the relative electrical power demand on the basis of this parameter and any thermal power required by the utility (in addition to that recovered by the PEMFCs) for heating needs during the heating period only. The auxiliary vapor compression electric cooling machine was modelled assuming a constant SEER value of 5 and, therefore, calculating the relative electrical power demand on the basis of this parameter and any cooling power required by the airport (in addition to that generated by the ADCH fed by the seasonal thermal storage) for space cooling during the cooling period only.
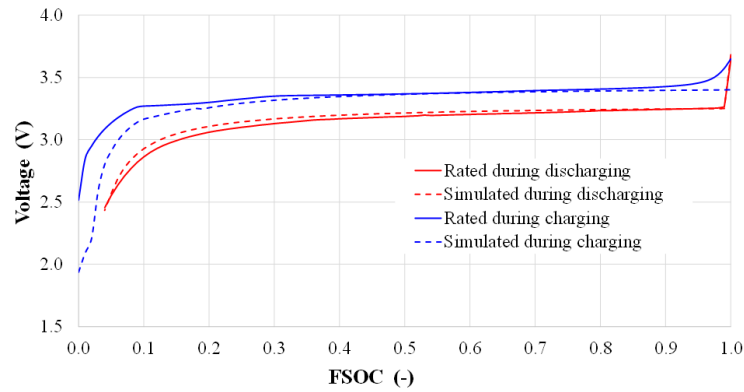

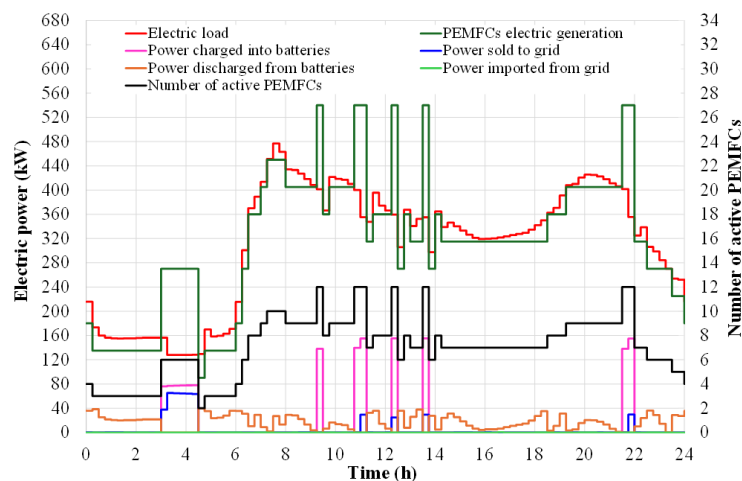**Figure 7.** Simulated vs. rated performance of a single cell of the batteries

Figure 8. Typical daily operation of PEMFCs and batteries

5 Simulation Results and Discussion

The system described in sections 3 and 4 has been simulated over an entire year by using a simulation time-step of 1 minute. This section describes the simulation results and compares the performance of the proposed "Hydro-Gen"

system against a baseline scenario (assumed as reference) from energy and economic points of view. In particular, the proposed system has been simulated under two different operating scenarios:

1) Scenario 1: thermal energy cogenerated by the PEMFCs is totally dissipated via the air-to-water heat exchangers;

2) Scenario 2: thermal energy cogenerated by the PEMFCs is exploited as much as possible for heating purposes as well as for activating the adsorption chiller; the remaining portion is eventually dissipated.

Figure 9 highlights the annual electric energy flows of the proposed "Hydro-Gen" system under both the above-mentioned operating scenarios. In particular, PEMFCs cogenerated electricity, cogenerated electricity charged into batteries, cogenerated electricity discharged from batteries, cogenerated electricity sold to the grid, electricity imported from the grid, electricity demand of the auxiliary heating system, electricity demand of the auxiliary cooling system, electric load of the airport without considering the auxiliary heating and cooling systems, as well as the total electric load of the airport are reported. Figure 9 indicates that:

• The total electric annual load of the airport represents about 98.7% and 97.7%, respectively, of the annually cogenerated electricity in scenario 1 and 2;

• The exploitation of annually cogenerated thermal energy (scenario 2) reduces, with respect to the scenario 1, the annual electrical energy required by the auxiliary heating system by 73.0%, the annual electrical energy consumed by the auxiliary cooling system by 43.6%, the annual total electrical load by 14.8% and, therefore, the annual hydrogen consumption by 16.7% (from 2.27 NMm^3/year to 1.89 NMm^3/year);

• About 5.0% and 6.2% of the annually electrical energy cogenerated is stored in the batteries in scenarios 1 and 2, respectively;

• 1.0% and 1.2% of the annual cogenerated electricity is transferred to the grid in scenarios 1 and 2, respectively. In both scenarios the central grid is not needed as back-up system.
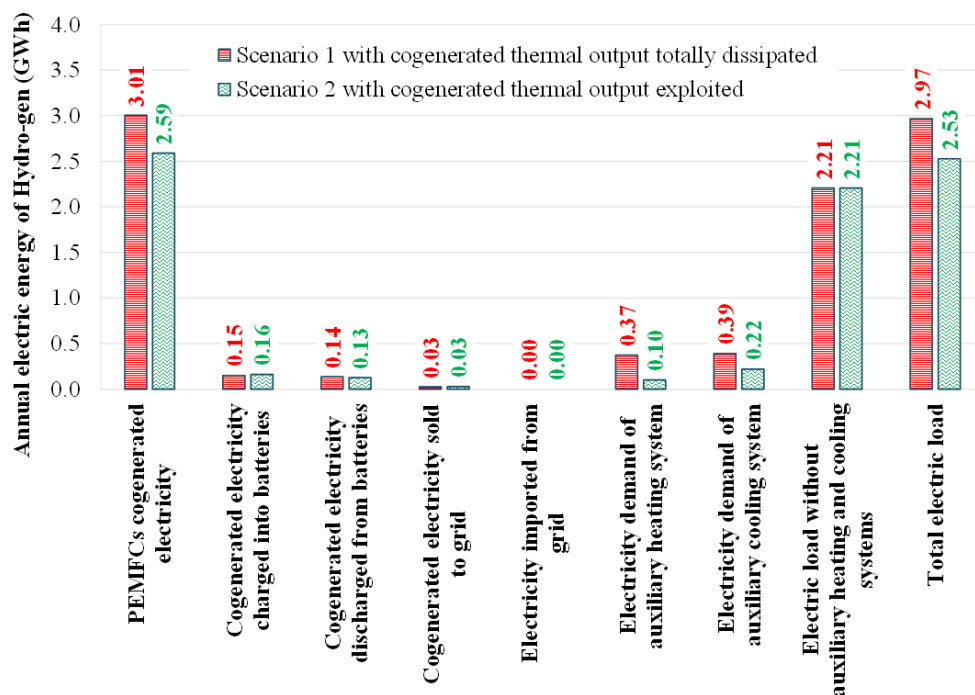

Figure 9. Annual electric energy flows under both scenarios

Figure 10 shows the annual thermal and cooling energy flows of the "Hydro-Gen" system. In particular, the annual PEMFCs cogenerated thermal output, dissipation of cogenerated thermal output, cogenerated thermal output stored in the tank, cogenerated thermal output used for heating, cogenerated thermal output used for feeding the ADCH, cooling energy supplied by the ADCH, thermal output of the auxiliary heating system and cooling output of the auxiliary cooling system are reported.

This figure underlines that:

• The thermal energy annually cogenerated by the PEMFCs corresponds to 91.5% of the annually cogenerated electric energy in scenario 2 (Figure 9);

• In scenario 2 the cogenerated thermal energy is totally used without dissipation;

• 100.0% of thermal energy annually cogenerated by the PEMFCs is stored in the thermal energy storage in scenario 2, of which 40.5% is used for heating purposes and 59.5% to thermally power the ADCH;
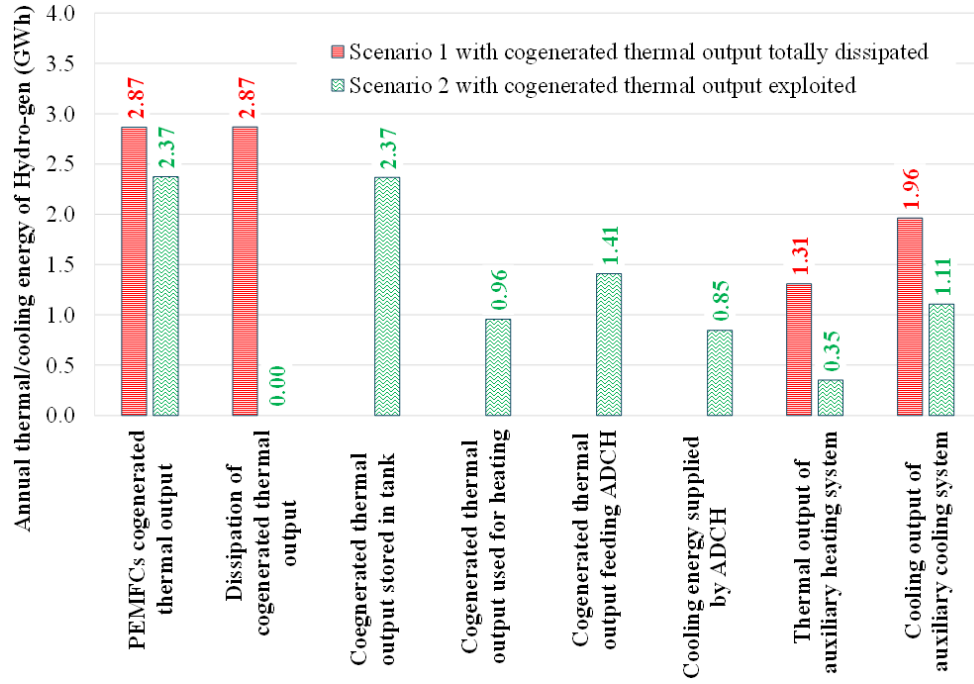
Figure 10. Annual thermal/cooling energy flows under both scenarios

• 73.3% of the annual airport's thermal energy demand is covered by the PEMFCs in scenario 2 (the remaining part is covered by the auxiliary heating system);

• 43.4% of the annual airport's cooling demand is satisfied via the ADCH thermally powered by the thermal output of the PEMFCs in scenario 2 (the remainder is met by the auxiliary cooling system).

In this study, operating scenarios 1 and 2 of the "Hydro-Gen" system are compared with a baseline scenario (assumed as reference) from energy and economic points of view. In greater detail, in the case of the baseline scenario, the total electric demand is completely covered via the central electric grid, the overall thermal demand for heating purposes is totally satisfied by means of an air-to-water vapor compression electric heat pump with a constant SCOP equal to 3.5, and the total cooling demand for space cooling is fully obtained through an air-to-water vapor compression electric refrigerating machine with a constant SEER equal to 5. According to reference [8], the following parameters have been calculated to compare the energy and economic performance of the proposed "Hydro-Gen" system in contrast with those of the baseline scenario while serving the same airport:

$$PE_{BS} = \frac{E_{el,load,w/oHVAC}}{\eta_{el,ref}} + \frac{E_{th,load}}{SCOP \cdot \eta_{el,ref}} + \frac{E_{cool,load}}{SEER \cdot \eta_{el,ref}} \tag{1}$$

$$PE_{Hydro\text{-}Gen} = \frac{E_{el,imported} - E_{el,sold}}{\eta_{el,ref}} \tag{2}$$

$$PES = \frac{PE_{BS} - PE_{Hydro\text{-}Gen}}{PE_{BS}} \tag{3}$$

$$OC_{BS} = \left(E_{el,load,w/oHVAC} + \frac{E_{th,load}}{SCOP} + \frac{E_{cool,load}}{SEER} \right) \cdot UC_{el,imported} \tag{4}$$

$$OC_{Hydro\text{-}Gen} = E_{el,imported} \cdot UC_{el,imported} + mH_2 \cdot UCH_2 - E_{el,sold} \cdot UP_{el,sold} \tag{5}$$

$$\Delta OC = \frac{OC_{BS} - OC_{Hydro\text{-}Gen}}{OC_{BS}} \tag{6}$$

where, PE_{BS} is the annual primary energy consumption of the baseline scenario, $PE_{\text{Hydro-Gen}}$ is annual primary energy consumption associated to the operation of the "Hydro-gen" system, PES is annual primary energy saving, OC_{BS} is the annual operating cost of the baseline scenario, $OC_{\text{Hydro-Gen}}$ is the annual operating cost associated to the operation of the "Hydro-Gen" system, ΔOC is percentage difference between the baseline scenario and the "Hydro-Gen" system, $E_{\text{el,load,w/oHVAC}}$ is the annual electric energy demand of the airport excluding the consumption associated to the operation of heating and cooling systems, $\eta_{\text{el,ref}}$ is the average efficiency of the central grid, $E_{\text{th,load}}$ is the annual thermal demand of the airport for heating purposes, $E_{\text{cool,load}}$ is the annual cooling demand of the airport for space cooling, $E_{\text{el,imported}}$ is the annual electric energy imported/purchased from the central grid, $E_{\text{el,sold}}$ is the annual electric energy exported/sold to the central grid, $UC_{\text{el,imported}}$ is the unit cost of electricity purchased from the grid, $UP_{\text{el,sold}}$ is unit price of electricity sold to the grid, mH_2 is the mass of hydrogen consumed by the "Hydro-Gen" system and UCH_2 is unit cost of green hydrogen. Eqs. (1)–(6) have been derived by assuming that the required amount of hydrogen is totally obtained by using an electrolyzer driven by renewable electricity (therefore, it has been assumed that hydrogen production is without primary consumption). Cardona et al. [8], suggested that the parameter $\eta_{\text{el,ref}}$ has been assumed equal to 0.42, while $UC_{\text{el,imported}}$ and $UP_{\text{el,sold}}$ have been considered equal to 0.18 €/kWh and 0.06 €/kWh, respectively. Janssen et al. [20] investigated the production of renewable hydrogen in 30 European countries via solar, onshore wind, and curtailed offshore wind electricity, or a combination of these generation options; in the short-term, the study estimated a levelized cost of hydrogen equal to 3.50 ÷ 15.00 €/kg, 3.00 ÷ 4.00 €/kg and 3.20 ÷ 8.00 €/kg for solar PV, onshore wind, and curtailed offshore wind, respectively.

The results showed that, according to Eqs. (1)–(3), the proposed "Hydro-Gen" system allows to annually save a significant amount of primary energy (from a minimum of 100.8% in the case of the scenario 1 up to a maximum of 100.9% in the case of the scenario 2) in comparison to the baseline scenario. The difference between scenarios 1 and 2 is negligible due to the fact that the amount of hydrogen required by the "Hydro-Gen" system is totally produced by means of renewable sources, thus obtained for free without consuming primary energy. Figure 11 reports the values of ΔOC (Eq. (6)) as a function of the operating scenario upon varying the unit cost of green hydrogen (that has been assumed in this paper ranging from 3.00 up to 15.00 €/kg [20]).
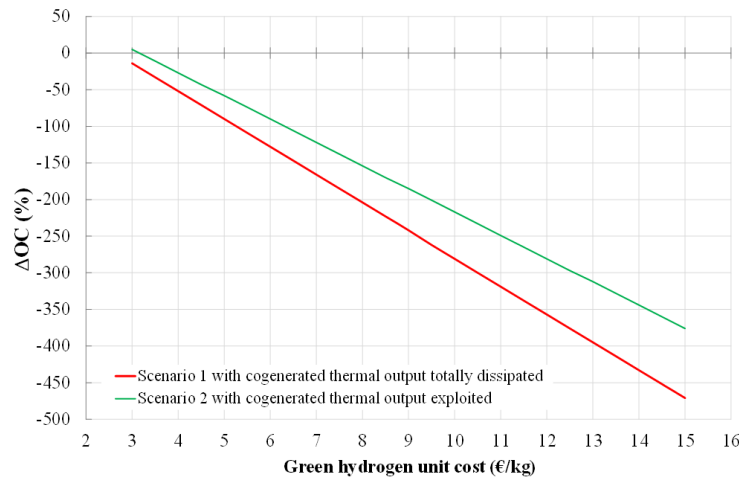

Figure 11. ΔOC upon varying the unit cost of green hydrogen

This figure underlines that the values of ΔOC range from –14% up to –472% in the case of the scenario 1 and between 5% and –376% in the case of the scenario 2; therefore, the values of ΔOC can achieve maximum values of –14% and 5% in the case of the scenario 1 and 2, respectively. In addition, this figure indicates that, for a given unit cost of green hydrogen, the scenario 2 of the "Hydro-Gen" system is characterized by better performance with respect to the scenario 1, with differences ranging from 19% up to 96%; this difference is due to the fact that in the case of the scenario 2 the cogenerate thermal output is effectively exploited. Positive values of ΔOC means that the proposed "Hydro-Gen" system reduces the operating costs with respect to the baseline scenario; according to Figure 11 the "Hydro-Gen" system can reduce the operating costs only in the scenario 2 when the unit cost of green hydrogen is less 3.16 €/kg. In the case of the scenario 1, the operating costs of the "Hydro-Gen" system becomes lower than those of the baseline scenario (i.e., ΔOC becomes positive) only if the unit cost of green hydrogen becomes lower than 2.63 €/kg (this value is currently lower than the minimum unit cost of green hydrogen [20]).

6 Conclusions

In this paper, the performance of an innovative containerized modular trigeneration system (based on fuel cells powered by hydrogen), named "Hydro-Gen", is numerically investigated by using the TRNSYS software

while serving a small-medium scale airport. The system has been simulated over a one-year period under two operational scenarios: scenario 1, where the cogenerated thermal energy is totally dissipated, and scenario 2, where the cogenerated thermal energy is effectively utilized to meet demand. Energy and economic performance have been analyzed and compared with a baseline scenario relying solely on power from the central grid. The results demonstrated that the proposed system significantly reduces primary energy consumption in both scenarios (achieving up to 100.9% savings) compared to the baseline (by assuming that hydrogen is totally produced via renewable energy sources). The proposed system is able to decrease the operating costs (up to a maximum of 5%) with respect to the baseline configuration only in the case of the operational scenario 2 with a unit cost of hydrogen lower than 3.16 €/kg. The simulation outputs underlined that scenarios 1 and 2 are characterized by similar performance in terms of primary energy demand, while the scenario 2 denoted better results from an economic point of view than the scenario 1 (with difference between from 19% to 96%).

Data Availability

The data used to support the findings of this study are available from the corresponding author upon request.

Conflicts of Interest

The authors declare that they have no conflicts of interest.

References

[1] L. M. Blanes, A. Costa, and M. M. Keane, "Simulation to support ISO 50001 energy management systems and fault detection and diagnosis. Case study of Malpensa airport," in *Proceedings of BS2013: 13th Conference of International Building Performance Simulation Association*, Chambéry, France, 2013, pp. 2100–2107.

[2] S. O. Alba and M. Manana, "Energy research in airports: A review," *Energies*, vol. 9, no. 5, p. 349, 2016. https://doi.org/10.3390/en9050349

[3] S. O. Alba and M. Manana, "Characterization and analysis of energy demand patterns in airports," *Energies*, vol. 10, no. 1, p. 119, 2017. https://doi.org/10.3390/en10010119

[4] S. Sibilio, A. Rosato, G. Ciampi, M. Scorpio, and A. Akisawa, "Building-integrated trigeneration system: Energy, environmental and economic dynamic performance assessment for Italian residential applications," *Renew. Sustain. Energy Rev.*, vol. 68, pp. 920–933, 2017. https://doi.org/10.1016/j.rser.2016.02.011

[5] A. Rosato and S. Sibilio, "Preliminary experimental characterization of a three-phase absorption heat pump," *Int. J. Refrig.*, vol. 36, no. 3, pp. 717–729, 2013. https://doi.org/10.1016/j.ijrefrig.2012.11.015

[6] A. Rosato, A. Ciervo, F. Guarino, G. Ciampi, M. Scorpio, and S. Sibilio, "Dynamic simulation of a solar heating and cooling system including a seasonal storage serving a small Italian residential district," *Therm. Sci.*, vol. 24, no. 6 Part A, pp. 3555–3568, 2020. https://doi.org/10.2298/TSCI200323276R

[7] G. Ciampi, A. Rosato, S. Sibilio, E. Entchev, and W. Yaici, "Parametric analysis of solar heating and cooling systems for residential applications," *Heat Transf. Eng.*, vol. 41, no. 12, pp. 1052–1074, 2020. https://doi.org/10.1080/01457632.2019.1600873

[8] E. Cardona, A. Piacentino, and F. Cardona, "Energy saving in airports by trigeneration. Part I: Assessing economic and technical potential," *Appl. Therm. Eng.*, vol. 26, no. 14-15, pp. 1427–1436, 2006. https://doi.org/10.1016/j.applthermaleng.2006.01.019

[9] F. Calise, F. L. Cappiello, L. Cimmino, and M. Vicidomini, "Dynamic simulation modelling of reversible solid oxide fuel cells for energy storage purpose," *Energy*, vol. 260, p. 124893, 2022. https://doi.org/10.1016/j.energy.2022.124893

[10] P. E. V. de Miranda, "Hydrogen energy: Sustainable and perennial," in *Science and Engineering of Hydrogen-Based Energy Technologies*, 2019, pp. 1–38. https://doi.org/10.1016/B978-0-12-814251-6.00001-0

[11] University of Wisconsin—Madison, "A TRaNsient SYstems Simulation Program (TRNSYS 18)," 2017. https://sel.me.wisc.edu/trnsys/

[12] A. Rosato, A. Ciervo, G. Ciampi, M. Scorpio, F. Guarino, and S. Sibilio, "Energy, environmental and economic dynamic assessment of a solar hybrid heating network operating with a seasonal thermal energy storage serving an italian small-scale residential district: Influence of solar and back-up technologies," *Therm. Sci. Eng. Prog.*, vol. 19, p. 100591, 2020. https://doi.org/10.1016/j.tsep.2020.100591

[13] F. Ceglia, A. Macaluso, E. Marrasso, C. Roselli, and L. Vanoli, "Energy, environmental, and economic analyses of geothermal polygeneration system using dynamic simulations," *Energies*, vol. 13, no. 18, p. 4603, 2020. https://doi.org/10.3390/en13184603

[14] "AENA airport website." https://www.aena.es/en/seve-ballesteros-santander.html

[15] R. O'Hegarty, O. Kinnane, D. Lennon, and S. Colclough, "Air-to-water heat pumps: Review and analysis of the performance gap between in-use and product rated performance," *Renew. Sustain. Energy Rev.*, vol. 155, p. 111887, 2022. https://doi.org/10.1016/j.rser.2021.111887

[16] M. T. Ali and P. Armstrong, "Industry/government/academia partner to achieve SCOP> 5 hot-climate MEPS air-cooled chiller," *ASHRAE Trans.*, vol. 125, no. 1, pp. 368–376, 2019. https://doi.org/10.26190/unsworks/27704

[17] A. Rosato, F. Guarino, S. Sibilio, E. Entchev, M. Masullo, and L. Maffei, "Healthy and faulty experimental performance of a typical HVAC system under italian climatic conditions: Aartificial neural network-based model and fault impact assessment," *Energies*, vol. 14, no. 17, p. 5362, 2021. https://doi.org/10.3390/en14175362

[18] A. Rosato, M. E. Youssef, H. Daoud, A. Al-Salaymeh, and M. G. Ghorab, "TRNSYS dynamic digital twin of hot and cold sensible thermal energy storages: An experimental calibration and validation approach," *J. Energy Storage*, vol. 105, p. 114700, 2025. https://doi.org/10.1016/j.est.2024.114700

[19] G. Restuccia, A. Freni, S. Vasta, and Y. Aristov, "Selective water sorbent for solid sorption chiller: Experimental results and modelling," *Int. J. Refrig.*, vol. 27, no. 3, pp. 284–293, 2004. https://doi.org/10.1016/j.ijrefrig.2003.09.003

[20] J. L. Janssen, M. Weeda, R. J. Detz, and B. van der Zwaan, "Country-specific cost projections for renewable hydrogen production through off-grid electricity systems," *Appl. Energy*, vol. 309, p. 118398, 2022. https://doi.org/10.1016/j.apenergy.2021.118398